



Lasers in Manufacturing Conference 2015

## Laser-Induced Subsurface Modification of Silicon Wafers

Paul Verburg<sup>a,b,\*</sup>, Lachlan Smillie<sup>c</sup>, Gert-Willem Römer<sup>a</sup>, Bianca Haberl<sup>c,d</sup>, Jodie Bradby<sup>c</sup>, Jim Williams<sup>c</sup>, Bert Huis in 't Veld<sup>a</sup>

<sup>a</sup>University of Twente, Faculty of Engineering Technology, Chair of Applied Laser Technology, P.O. Box 217, 7500 AE Enschede, The Netherlands.

<sup>b</sup>Present address: ASM Laser Separation International B.V., Platinawerf 20-G, 6641 TL Beuningen, The Netherlands.

<sup>c</sup>Research School of Physics and Engineering, The Australian National University, Acton, ACT 2601, Australia.

<sup>d</sup>Present address: Chemical and Engineering Materials Division, Oak Ridge National Laboratory, Oak Ridge, TN 37831, USA.

---

### Abstract

In addition to the processing of transparent dielectric materials, pulsed lasers can be used to produce subsurface modifications inside silicon by employing near- to mid-infrared light. An application of these modifications is laser-induced subsurface separation, which is a method to separate wafers into individual dies. We investigated the subsurface modification process using a combination of numerical simulations and experiments. Different wavelengths, pulse durations and pulse energies were tested. We found that subsurface melting of silicon followed by rapid resolidification is the primary material modification mechanism. Lattice defects and transformations to both amorphous silicon and pressure-induced high density silicon phases occurred as a result of the laser irradiation.

Silicon, subsurface, wafer dicing, laser-material interaction, electron microscopy.

---

### 1. Introduction

Laser-induced subsurface separation is a two-step process to separate wafers into individual dies (Ohmura et al., 2006). First, tracks of subsurface modifications are created inside the wafer. Secondly, an external force is exerted on the wafer to fracture it along the subsurface modifications. An example of a sidewall of a separated die is shown in Fig. 1. Advantages of this wafer separation method are that it is dry and nearly debris-free. Other potential applications of subsurface modifications in silicon are the production of optical components (Nejadmalayeri et al., 2005) and resistivity tuning (Boulais et al., 2011). In this paper, we discuss the formation mechanism of laser-induced subsurface modifications in crystalline silicon, based on numerical simulations and experiments.

---

\* Corresponding author. Tel.: +31 (0)24 678 28 91.  
E-mail address: pverburg@alsi.asmt.com.

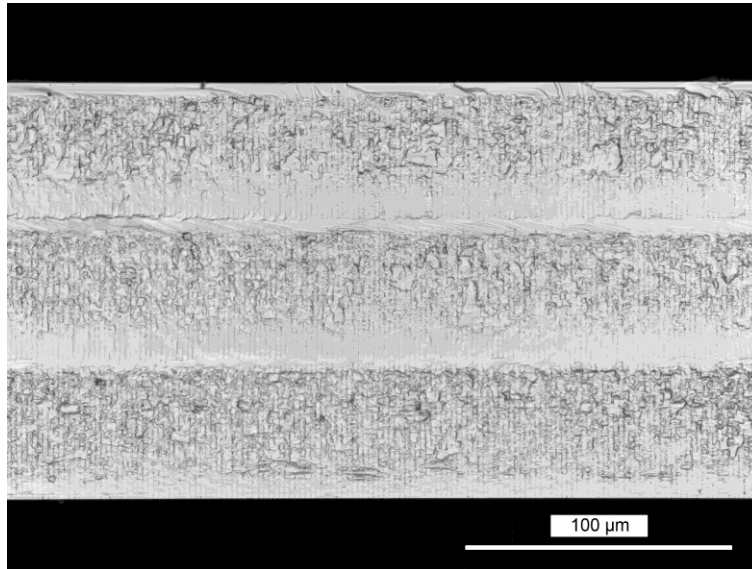


Fig. 1. Laser scanning confocal micrograph of a fracture plane obtained after dicing a 160- $\mu\text{m}$  thick silicon wafer (Verburg, 2015). Wavelength: 1549 nm, pulse energy: 2  $\mu\text{J}$ , pulse duration: 3.5 ns, transverse spacing modifications: 2  $\mu\text{m}$ . Three different focus depths inside the wafer were employed. The laser beam propagation direction is from top to bottom.

## 2. Numerical simulations and model validation

The laser-material interaction during the formation of laser-induced subsurface modifications in silicon was investigated by combining a two-temperature model with a non-linear Schrödinger equation to model the propagation of the laser beam (Verburg, 2014; Verburg, 2015). The numerical model simulates the distributions of the lattice temperature, electron temperature, carrier density and laser intensity as a function of time during the pulse. Single, two-photon and free-carrier absorption were included as were refractive index gradients due to the optical Kerr effect and variations in temperature and carrier density. Moreover, diffusion of heat and free carriers were accounted for. An example of a distribution of the maximum lattice temperatures that were reached during the laser pulse is shown in Fig. 2. The area that is plotted in black reached the liquid phase. To predict the dimensions of the subsurface modifications, it was assumed that the material that has been molten during the laser pulse will not regain its original almost defect-free crystalline structure after resolidification.

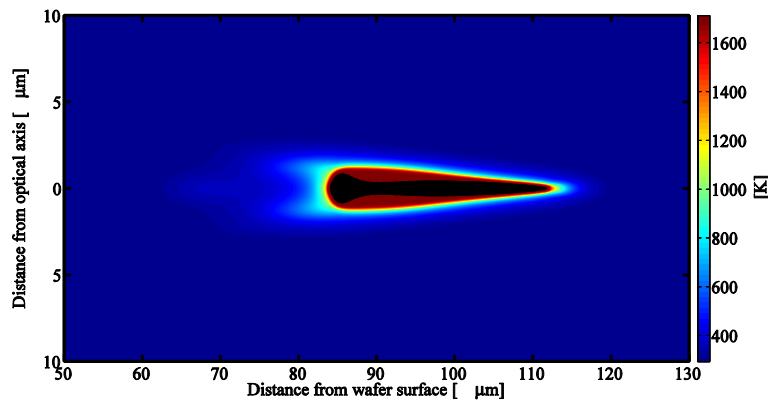


Fig. 2. Cross-section of the maximum lattice temperatures [K] during a laser pulse (Verburg, 2015). Wavelength: 1550 nm, pulse energy: 1  $\mu\text{J}$ , pulse duration: 1 ns, focus depth: 100  $\mu\text{m}$ , numerical aperture: 0.7, Gaussian beam with  $1/e^2$  contour filling 80% of the aperture. The beam propagation direction is from left to right.

Based on the simulation results, two strategies were found to be suitable for the production of subsurface modifications in silicon. The first strategy requires a laser wavelength around 1064 nm, resulting in a photon energy that is close to the band-gap of silicon. Since the linear interband absorption coefficient of silicon increases with temperature, a

thermal runaway can be triggered. The second strategy relies on a photon energy well-below the band-gap, which enables the use of multi-photon absorption to selectively absorb the laser energy below the surface. For this strategy, a wavelength of 1550 nm was selected.

The 1550 nm process requires pulse durations in the short nanosecond range to obtain effective two-photon absorption near the focus of the beam, when employing a focussing objective with a numerical aperture of 0.7 and a Gaussian laser beam. The 1064 nm process is also viable with longer nanosecond pulses. However, excessive conduction of heat and free carriers during the pulse should be prevented. Apart from an upper boundary, a lower boundary to the pulse duration was also found to exist. When using short picosecond pulses, the intensities throughout the path of the laser beam inside silicon are too high to limit the two-photon absorption to the vicinity of the focus of the laser beam. Instead, two-photon absorption takes place well-above the focal spot. Besides direct energy losses, this results in the generation of a dense electron-hole plasma, causing free-carrier absorption of laser energy and plasma defocussing before the laser beam reaches the location of the focus.

To validate the numerical results and the hypothesis that subsurface melting leads to the formation of modifications, three different laser sources were employed that provide 6.6 ps pulses at 1030 nm, 2-460 ns pulses (tunable) at 1061 nm and 3.5 ns pulses at 1549 nm. A Leica 11 101 666 infrared microscope objective with a cover correction for 100  $\mu\text{m}$  silicon was used to focus the laser pulses inside silicon samples. The presence of subsurface modifications was investigated in a non-destructive manner using infrared microscopy. Next, the dimensions of the modifications were measured by analysing the sidewalls of the dies that were formed by fracturing the samples along the subsurface modifications.

Both the 1061 and 1549 nm laser sources were successfully used to produce subsurface modifications. For the 1061 nm source, the full range of pulse durations of 2-460 ns was tested. All pulse durations were usable, although the range of suitable pulse energies was narrow for a pulse duration of 2 ns. At this duration, only on-sample pulse energies of approximately 0.15 to 0.9  $\mu\text{J}$  resulted in subsurface modifications. As predicted by the numerical model, the experiments using picosecond pulses did not yield modifications. Moreover, it was found that a good correlation exists between the simulated lengths of the volumes of molten material along the optical axis and the measured dimensions of the subsurface modifications on fracture planes (see Fig. 3). This suggests that the formation of a volume of liquid silicon below the surface is indeed required to induce a modification.

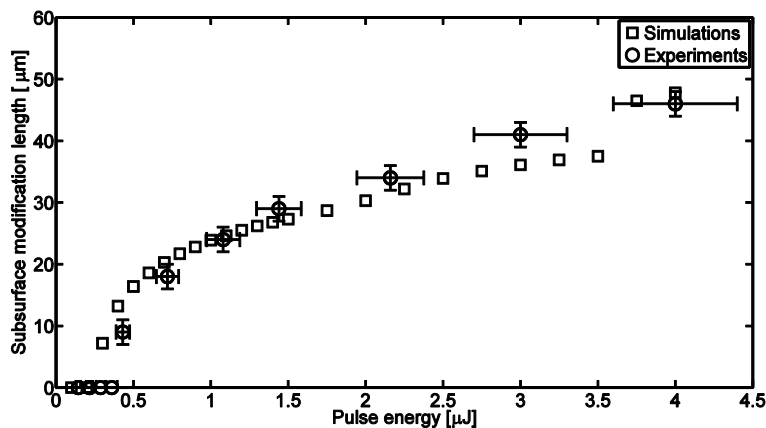


Fig. 3. Comparison of experimental and simulated modification lengths along the optical axis (Verburg, 2015). Wavelength: 1549 nm, pulse duration: 3.5 ns,  $M^2 = 1.1$ , focus depth: 100  $\mu\text{m}$ , numerical aperture: 0.7, Gaussian beam with  $1/e^2$  contour filling 80% of the aperture.

### 3. Analysis of the material structure of subsurface modifications

To establish the material structure of the subsurface modifications, scanning electron microscopy (SEM), Raman spectroscopy and transmission electron microscopy (TEM) were employed (Verburg et al., 2015). A SEM micrograph of a single track of subsurface modifications is shown in Fig. 4. Vertical lines corresponding to the spacing between the laser pulses can be observed as well as a number of voids. Since these voids suggest that the density of the material elsewhere in the bulk of the material has increased, high pressure phases may have been formed. To verify whether this is the case, the sidewalls of separated dies were analysed by Raman spectroscopy. A peak around a Raman shift of 360  $\text{cm}^{-1}$  was detected, which indicates that Si-III/XII phases are present (Domnich and Gogotsi, 2002).

Finally, electron-transparent lamellae were extracted from subsurface modifications, perpendicular to the optical axis of the laser beam. A combination of mechanical polishing and focussed ion beam milling was employed for this purpose. A

TEM micrograph obtained from one of these lamellae can be found in Fig. 5. A square pattern consisting of amorphous material is visible that coincides with the optical axis of the laser beam. Other lamellae contained crystalline material with defects at the same location. Four defect lines radiate out of the corners of the square pattern. Between the defect lines, crystalline silicon with the same orientation as the original wafer is present. Additionally, bend contours are visible.

The features that were observed in this TEM lamella can be explained based on resolidification of a subsurface melt. Initially, epitaxial growth seeded by the unmodified material is expected to take place along  $\langle 100 \rangle$  directions. The defect lines are formed where adjacent  $\{100\}$  solidification fronts overlap. The speed of the resolidification fronts increases as they progress inwards, until the speed is too high to sustain defect-free crystal growth. Consequently, a square pattern of amorphous material or crystalline material with defects is left behind.

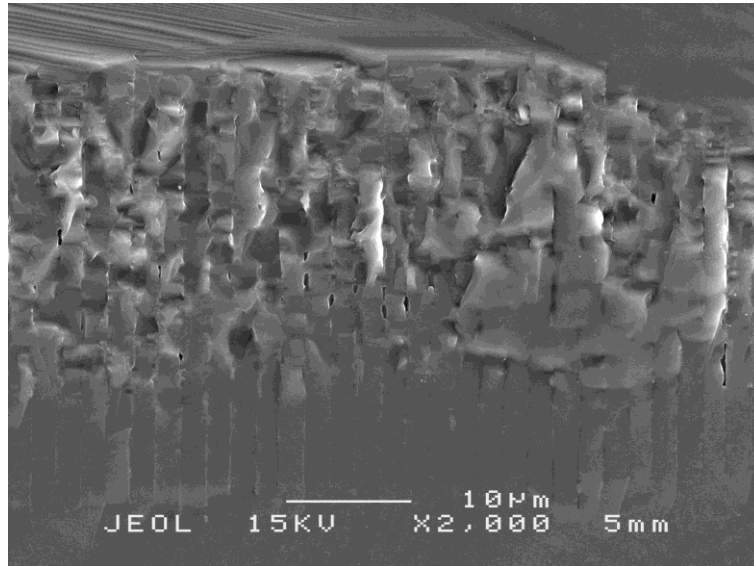


Fig. 4. SEM micrograph (secondary electrons) of a fracture plane obtained after dicing a 160- $\mu\text{m}$  thick silicon wafer (Verburg, 2015). Wavelength: 1549 nm, pulse duration: 3.5 ns, pulse energy: 1.3  $\mu\text{J}$ , transverse spacing modifications: 2  $\mu\text{m}$ . The laser beam propagation direction is from top to bottom.

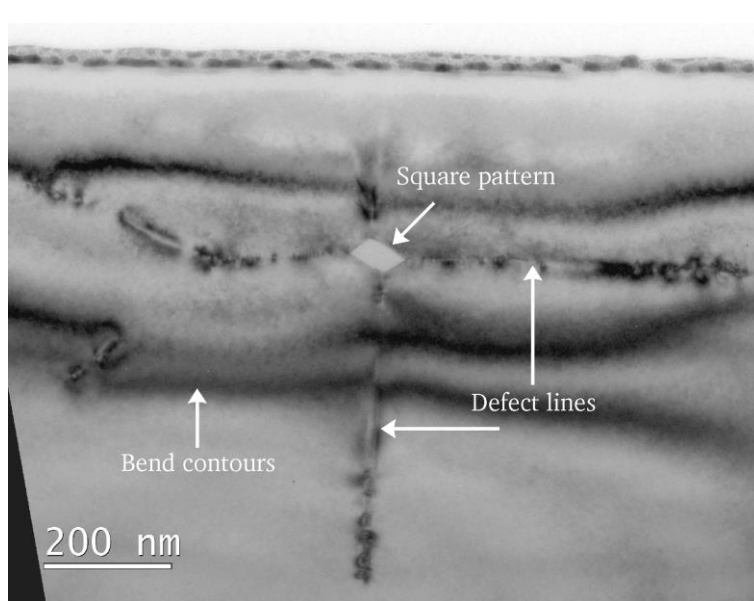


Fig. 5. TEM micrograph of a subsurface modification in silicon. Cross-section: perpendicular to the optical axis. Wavelength: 1549 nm, pulse duration: 3.5 ns, pulse energy: 2  $\mu\text{J}$ .

#### 4. Conclusions

We investigated the formation mechanism of laser-induced subsurface modifications in crystalline silicon. Based on numerical simulations of the laser-material interaction and the analysis of modifications by electron microscopy, it was found that subsurface melting and fast resolidification is the primary material modification mechanism. The crystalline silicon was transformed into amorphous silicon or crystalline silicon with defects as a result of the laser irradiation. Moreover, high pressure Si-III/XII phases were found. By simulating whether subsurface melting occurs, it was found to be possible to predict what laser parameters are suitable to produce subsurface modifications.

#### References

- Boulais, E., Fantoni, J., Chateauf, A., Savaria, Y., Meunier, M., 2011. Laser-Induced Resistance Fine Tuning of Integrated Polysilicon Thin-Film Resistors, *IEEE Transactions on Electron Devices* 58(2), p. 572.
- Domnich, V., Gogotsi, Y., 2002. Phase transformations in silicon under contact loading, *Reviews on Advanced Materials Science* 3, p. 1.
- Nejadmalayeri, A. H., Herman, P. R., Burghoff, J., Will, M., Nolte, S., Tünnermann, A., 2005. Inscription of optical waveguides in crystalline silicon by mid-infrared femtosecond laser pulses, *Optics Letters* 30(9), p. 964.
- Ohmura, E., Fukuyo, F., Fukumitsu, K., Morita, H., 2006. Internal Modified-Layer Formation Mechanism into Silicon with Nanosecond Laser, *Journal of Achievements in Materials and Manufacturing Engineering* 17, p. 381.
- Verburg, P. C.; Römer, G. R. B. E., Huis in 't Veld, A. J., 2014. Two-temperature model for pulsed-laser-induced subsurface modifications in Si, *Applied Physics A: Materials Science & Processing* 114(4), p. 1135.
- Verburg, P.C., 2015. Laser-Induced Subsurface Modification of Silicon Wafers, PhD Thesis, DOI 10.3990/1.9789036538381.
- Verburg, P.C., Smillie, L.A., Römer, G.R.B.E., Haberl, B., Bradby, J.E., Williams, J.S., Huis in 't Veld, A.J., 2015. Crystal Structure of Laser-Induced Subsurface Modifications in Si, *Applied Physics A: Materials Science & Processing*, DOI 10.1007/s00339-015-9238-5.